Linking multiple relaxation, power-law attenuation, and fractional wave equations

Sven Peter Näsholm[a] and Sverre Holm
Department of Informatics, University of Oslo, P.O. Box 1080, NO-0316 Oslo, Norway

(Received 8 June 2011; revised 21 August 2011; accepted 31 August 2011)

The acoustic wave attenuation is described by an experimentally established frequency power law in a variety of complex media, e.g., biological tissue, polymers, rocks, and rubber. Recent papers present a variety of acoustical fractional derivative wave equations that have the ability to model power-law attenuation. On the other hand, a multiple relaxation model is widely recognized as a physically based description of the acoustic loss mechanisms as developed by Nachman *et al.* [J. Acoust. Soc. Am. **88**, 1584–1595 (1990)]. Through assumption of a continuum of relaxation mechanisms, each with an effective compressibility described by a distribution related to the Mittag-Leffler function, this paper shows that the wave equation corresponding to the multiple relaxation approach is identical to a given fractional derivative wave equation. This work therefore provides a physically based motivation for use of fractional wave equations in acoustic modeling.
 [DOI: 10.1121/1.3641457]

PACS number(s): 43.80.Cs, 43.20.Hq, 43.20.Jr, 43.20.Bi [TDM] Pages: 3038–3045

I. INTRODUCTION

This paper concerns acoustical wave modeling in lossy media where the attenuation follows a frequency power law. It provides an incentive to apply a fractional wave equation.

Acoustic wave attenuation in complex media like those encountered in medical ultrasound are often considered to be due to multiple relaxation mechanisms following the description of Nachman *et al.*[1] Their thorough work relies on thermodynamics and first principles of acoustical physics. The lossy wave equation of Ref. 1 for N relaxation mechanisms becomes a partial differential equation with its highest time derivative of order $N+2$. The reference also presents exact expressions for the frequency-dependent sound speed $c(\omega)$ and the attenuation $\alpha_k(\omega)$ as functions of each mechanism's compressibility and relaxation time. The wave equation is causal. Therefore, the attenuation is related to the sound-speed dispersion as described by the Kramers–Kronig relations.[2] For the rest of the present paper, this model will be denoted the Nachman–Smith–Waag (NSW) model.

For not so complex media, the different terms of the NSW attenuation can, under reasonable assumptions, be decoupled. Then the attenuation is of the form

$$\alpha_k = \sum_{\nu=1}^{N} \alpha_\nu \frac{\Omega_\nu \omega^2}{\omega^2 + \Omega_\nu^2}. \tag{1}$$

Incidentally, simple media with only a few clearly identifiable relaxation mechanisms, like air and salt water, are described by the same model. In both cases, $N=3$ processes are sufficient to describe the attenuation. For both media, the first term is made into a viscous attenuation term by demanding that $\omega \ll \Omega_1$ so that the first term becomes $\propto \omega^2$ for the frequencies of interest. The two other relaxation mechanisms in air are due to nitrogen and oxygen and the variation of the parameters with humidity and temperature has been described by Bass *et al.*[3] Likewise, in water, the first term is characteristic of distilled water, whereas salt water mainly adds two relaxation mechanisms, which are due to magnesium sulfate and boric acid. The parameter variation with temperature, salinity, *p*H, and depth is given by Ainslie and McColm.[4]

In more complex media, individual relaxation processes are not identifiable. The attenuation in biological tissue and other complex media such as polymers, rocks, and rubber often follows a power law in frequency: $\alpha_k(\omega) \propto \omega^\eta$, with the exponent between 0 and 2.[5] The range where experiments indicate such power laws to be valid may cover many frequency decades. In order to make the NSW model attenuation adequately follow ω^η, either the frequency band where it is valid must be narrow, or the number of assumed relaxation mechanisms N must be large.

The first way to deal with this is to restrict the frequency range and fit a model of low order N. This is the approach taken in Refs. 6 and 7 where models with $N=2$ or 3 are fitted to the desired attenuation characteristics. Parameter values are found from curve fitting and they do not really correspond to actual physical relaxation processes in the medium as in the air and salt water models.

The second approach is to require high-order wave equations with a high temporal derivative order. They may be cumbersome to apply to wave propagation model evaluation through analytical calculation or numerical simulation. Another problem is that as individual relaxation processes cannot be identified, it is nearly impossible to determine parameter values in such a model.

Disconnected from the NSW framework, other acoustical wave equations have been presented that consist of a d'Alambertian linear propagation component $\nabla^2 u - c_0^{-2}\partial^2 u/\partial t^2$ and one or several terms involving fractional derivatives. These terms make the wave equation able to model frequency power-law attenuation. The fractional derivative may either be spatial[8,9] or temporal.[10–15] For some, but not all, such wave equations, the Kramers–Kronig criterion is fulfilled therefore ensuring causality. However, the physical motivation for inclusion of temporal and/or spatial fractional derivative terms into the models just listed is for some of the references

[a]Author to whom correspondence should be addressed. Electronic mail: svenpn@ifi.uio.no

heuristic in view that the fractional derivative terms are added *ad hoc* in order to make the attenuation follow some power law corresponding to measurements. A more parsimonious way to derive a lossy linear wave equation is to start from the first physical principles of mass conservation and momentum conservation and combine it with some constitutive model relating stress and strain. This constitutive model may include fractional time derivatives, exemplified by Holm and Sinkus using the fractional Kelvin–Voigt constitutive model[14] and by Holm and Näsholm using the fractional Zener constitutive model.[15] The resulting lossy wave equations are causal and the corresponding attenuation follows power laws within wide frequency bands. As opposed to the fractional Kelvin–Voigt wave equation, the fractional Zener wave equation provides a frequency-dependent speed of sound that is finite for frequencies approaching infinity. A similar deduction of a nonlinear fractional wave equation is presented by Prieur and Holm in Ref. 16. Arbitrary attenuation power laws may also be derived from a constitutive stress–strain model described by a hierarchical fractal ladder network of springs and dashpots, as outlined in Ref. 17. The resulting power law is however valid only in the low-frequency regime and it includes a large number of degrees of freedom, which is unsuitable for parameter fits to measurement results.

In Ref. 18, Berkhoff *et al*. considered the NSW model for the case of a continuum of relaxation processes all of equal effective compressibility, being distributed logarithmically over a limited frequency band. Their resulting attenuation model appropriately fits experimental measurements for frequencies between 10 kHz and 100 MHz.

The purpose of the present paper is to establish a link between the NSW model and the fractional Zener model. This is done by assuming a continuum of relaxation mechanisms in the NSW model, however with a different effective compressibility weighting approach compared to the one used by Berkhoff *et al*. An expression for the corresponding generalized time-domain compressibility is obtained. This is compared to the generalized compressibility of the fractional Zener model. The conditions for these compressibilities to be equal are then investigated. The aim is to achieve a joint description where the advantages of the fractional Zener model are combined with those of the NSW model.

This paper is organized as follows. The theory section (Sec. II) first reviews the NSW model and the fractional Zener model. Then the section proceeds with the main contribution of this work where the connection between the two models is established by analysis of a model named the Mittag-Leffler distribution Nachman–Smith–Waag (ML-NSW) model. Section III provides a numerical model example regarding an attenuation power law with the exponent 1.1. Discussions and conclusions are given in Sec. IV. The paper closes with an appendix on the Mittag-Leffler function.

II. THEORY

A. The NSW model generalized to a continuum of relaxation mechanisms

The dispersion relation between the complex wavenumber k and the angular frequency ω is a spatiotemporal frequency domain representation of the wave equation. Using the generalized compressibility $\kappa(\omega)$, it may be written

$$k^2(\omega) = \omega^2 \rho_0 \kappa(\omega). \tag{2}$$

From the real and imaginary parts of the complex wavenumber, the frequency-dependent attenuation $\alpha_k(\omega)$ and speed of sound $c(\omega)$ may be found using

$$k^2(\omega) = \frac{\omega}{c(\omega)} - i\alpha_k(\omega). \tag{3}$$

The NSW model of Ref. 1 considers a general discrete set of relaxation mechanisms $\nu = 1,\ldots,N$, each with the corresponding relaxation time $\tau_1,\ldots,\tau_N$ and effective compressibility $\kappa_1,\ldots,\kappa_N$. For the temporal Fourier transform defined with the kernel $e^{-i\omega t}$, the total frequency-domain compressibility then becomes

$$\kappa(\omega) = \kappa_0 - i\omega \sum_{\nu=1}^{N} \frac{\kappa_\nu \tau_\nu}{1 + i\omega\tau_\nu}. \tag{4}$$

When solving for the attenuation under the reasonable assumption that $\kappa_\nu \ll \kappa_0$, the cross terms in the attenuation expression disappear and the decoupled equation (1) is obtained.

The zero-frequency compressibility κ_0 is given by $\kappa_0 \triangleq 1/(c_0^2\rho_0)$, where c_0 and ρ_0 are the steady-state sound speed and density.

In the following, a continuum of relaxation mechanisms is considered. The mechanisms are evenly distributed along the relaxation frequency axis Ω, whereas the associated effective compressibility is assumed to be some function of the relaxation frequency: $\kappa_\nu(\Omega)$.

Then the sum in Eq. (4) over the relaxation mechanisms turns to an integral over the relaxation frequency continuum in the band $\Omega \in [\Omega_1, \Omega_2]$, each with the relaxation time $\tau_\nu(\Omega) = 1/\Omega$. The relaxation frequency band might also cover $\Omega \in [0, \infty]$. The integral version of Eq. (4) thus becomes

$$\kappa(\omega) = \kappa_0 - i\omega \int_{\Omega_1}^{\Omega_2} \frac{\kappa_\nu(\Omega)}{\Omega + i\omega} \mathrm{d}\Omega \triangleq \kappa_\mathrm{N}(\omega). \tag{5}$$

Inverse Fourier transformation gives the time-domain generalized compressibility corresponding to the NSW relaxation model for a continuum of effective compressibilities:

$$\begin{aligned} \kappa_\mathrm{N}(t) &= \kappa_0\delta(t) - \frac{\mathrm{d}}{\mathrm{d}t}\left[H(t)\int_{\Omega_1}^{\Omega_2} e^{-t\Omega}\kappa_\nu(\Omega)\,\mathrm{d}\Omega\right] \\ &= \delta(t)\left[\kappa_0 - \int_{\Omega_1}^{\Omega_2} \kappa_\nu(\Omega)\,\mathrm{d}\Omega\right] \\ &\quad - H(t)\frac{\mathrm{d}}{\mathrm{d}t}\left[\int_{\Omega_1}^{\Omega_2} e^{-t\Omega}\kappa_\nu(\Omega)\,\mathrm{d}\Omega\right], \end{aligned} \tag{6}$$

where $H(t)$ is the Heaviside step function, $\delta(t)$ is the Dirac delta function, and the relation $\delta(t)e^{-\Omega t} = \delta(t)$ is used. One may note that the integral in the equation above has the structure of a Laplace transform.

Reference 1 defines the infinite-frequency generalized compressibility κ_∞, which for case (5) of a continuum of relaxation mechanisms turns into

$$\kappa_\infty \triangleq \kappa_0 - \int_{\Omega_1}^{\Omega_2} \kappa_\nu(\Omega)\,\mathrm{d}\Omega. \tag{7}$$

B. The fractional Zener model

This section mainly reviews relevant results from Ref. 15 regarding the fractional Zener wave equation.

1. Stress–strain relation and generalized compressibility

The following equation gives a representation of the fractional Zener stress–strain constitutive relation as expressed by Bagley and Torvik in Ref. 19, Eq. (3):

$$\sigma(t) + \tau_\epsilon^\beta \frac{\partial^\beta \sigma(t)}{\partial t^\beta} = E_0\left[\epsilon(t) + \tau_\sigma^\alpha \frac{\partial^\beta \epsilon(t)}{\partial t^\alpha}\right]. \tag{8}$$

The fractional Kelvin–Voigt stress–strain relation is obtained from Eq. (8) by setting $\tau_\epsilon = 0$.

The history of the fractional derivatives in physics goes back to 1826.[20] For a mathematical introduction, see, e.g., Ref. 21. Inclusion of fractional derivatives in the stress–strain relationship facilitates the description of materials where the response depends on the past history, see, e.g., Sec. II B of Ref. 9.

The frequency-domain representation of Eq. (8) is

$$\left[1 + (\tau_\epsilon i\omega)^\beta\right]\sigma(\omega) = E_0[1 + (\tau_\sigma i\omega)^\alpha]\epsilon(\omega). \tag{9}$$

From Eq. (9), the generalized compressibility $\kappa_Z(\omega) \triangleq \epsilon(\omega)/\sigma(\omega)$ may be expressed as

$$\kappa_Z(\omega) \triangleq \kappa_0 \frac{1 + (\tau_\epsilon i\omega)^\beta}{1 + (\tau_\sigma i\omega)^\alpha}, \tag{10}$$

where $E = 1/\kappa_0$. For the investigations to follow, it is convenient to write this as

$$\kappa_Z(\omega) = \kappa_0\left[\frac{\tau_\sigma^{-\alpha}}{\tau_\sigma^{-\alpha} + (i\omega)^\alpha} + i\omega\frac{\tau_\sigma^{-\alpha}\tau_\epsilon^\beta (i\omega)^{\beta-1}}{\tau_\sigma^{-\alpha} + (i\omega)^\alpha}\right]. \tag{11}$$

The inverse Fourier transform of Eq. (11) gives the causal time-domain generalized compressibility corresponding to the fractional Zener model.

As discussed in Ref. 15 based on arguments from Refs. 22 and 23, setting $\alpha = \beta$ ensures the stress relaxation to be monotonically decreasing. Helped by the Fourier transform relation in Eq. (A2), Eq. (11) may be expressed in terms of the Mittag-Leffler function $E_{\alpha,\beta}(t)$ as defined in the Appendix:

$$\begin{aligned}\kappa_Z(t) = {} & H(t)\left\{\frac{\kappa_0 t^{\alpha-1}}{\tau_\sigma^\alpha} E_{\alpha,\alpha}[-(t/\tau_\sigma)^\alpha]\right\} \\ & + \frac{\mathrm{d}}{\mathrm{d}t}\left\{\frac{\kappa_0\tau_\epsilon^\alpha}{\tau_\sigma^\alpha} H(t) E_{\alpha,1}[-(t/\tau_\sigma)^\alpha]\right\},\end{aligned} \tag{12}$$

which in view of Eq. (A4) becomes

$$\begin{aligned}\kappa_Z(t) = {} & H(t)\left\{-\kappa_0 \frac{\mathrm{d}}{\mathrm{d}t} E_{\alpha,1}[-(t/\tau_\sigma)^\alpha]\right\} + \frac{\mathrm{d}}{\mathrm{d}t}\left\{\frac{\kappa_0\tau_\epsilon^\alpha}{\tau_\sigma^\alpha} H(t) E_{\alpha,1}[-(t/\tau_\sigma)^\alpha]\right\} = -\kappa_0\left(1 - \tau_\epsilon^\alpha/\tau_\sigma^\alpha\right)H(t)\frac{\mathrm{d}}{\mathrm{d}t}E_{\alpha,1}[-(t/\tau_\sigma)^\alpha] \\ & + \frac{\kappa_0\tau_\epsilon^\alpha}{\tau_\sigma^\alpha}\delta(t) E_{\alpha,1}[-(t/\tau_\sigma)^\alpha] = \frac{\kappa_0\tau_\epsilon^\alpha}{\tau_\sigma^\alpha}\delta(t) - \kappa_0\left(1 - \tau_\epsilon^\alpha/\tau_\sigma^\alpha\right)H(t)\frac{\mathrm{d}}{\mathrm{d}t}E_{\alpha,1}[-(t/\tau_\sigma)^\alpha].\end{aligned} \tag{13}$$

2. Wave equation

By combining the fractional Zener constitutive stress–strain relation (8) with the equation for momentum conservation and the equation for linearized mass conservation, the following lossy fractional Zener wave equation may be deduced:

$$\nabla^2 u - \frac{1}{c_0^2}\frac{\partial^2 u}{\partial t^2} + \tau_\sigma^\alpha \frac{\partial^\alpha}{\partial t^\alpha}\nabla^2 u - \frac{\tau_\epsilon^\alpha}{c_0^2}\frac{\partial^{\alpha+2} u}{\partial t^{\alpha+2}} = 0. \tag{14}$$

This wave equation is causal and in the spatiotemporal frequency domain it corresponds to the following dispersion relation between k and ω:

$$k^2 = \frac{\omega^2}{c_0^2}\frac{1 + (\tau_\epsilon i\omega)^\alpha}{1 + (\tau_\sigma i\omega)^\alpha}. \tag{15}$$

3. Frequency-dependent attenuation and speed of sound

The expression for the fractional Zener complex wavenumber k given in Eq. (15) may be combined with Eq. (3) in order to yield the attenuation as

$$\alpha_{k,Z}(\omega) \triangleq -\Im\left\{\frac{\omega}{c_0}\sqrt{\frac{1 + (\tau_\epsilon i\omega)^\alpha}{1 + (\tau_\sigma i\omega)^\alpha}}\right\} \tag{16}$$

and the fractional Zener model speed of sound as

$$c_Z(\omega) \triangleq \Re\left\{c_0\left[\frac{1 + (\tau_\epsilon i\omega)^\alpha}{1 + (\tau_\sigma i\omega)^\alpha}\right]^{-1/2}\right\}. \tag{17}$$

The asymptotes of the attenuation is found to obey frequency power laws as $\alpha_k \propto \omega^{1+\alpha}$ in a low-frequency regime, $\alpha_k \propto$

$\omega^{1-\alpha/2}$ in an intermediate frequency regime, and $\alpha_k \propto \omega^{1-\alpha}$ in a high-frequency regime.

The fractional Zener model fits measurements well and is characterized by a relatively small number of parameters. Both properties are advantages compared to the NSW model. The fractional Zener model also satisfies basic physical requirements like causality and finite sound speed for all frequencies. Nevertheless it is not possible to derive the parameter values from basic physics. In the section that follows we will provide a connection between the fractional Zener model and the physically somewhat more intuitive multiple relaxation NSW model.

C. Continuum of NSW relaxation mechanism distribution resulting in the fractional Zener model

The NSW multiple-relaxation generalized compressibility $\kappa_N(t)$ and the fractional Zener generalized compressibility $\kappa_Z(t)$ given by Eqs. (6) and (13) are equal when

$$\delta(t)\left[\kappa_0-\int_{\Omega_1}^{\Omega_2}\kappa_\nu(\Omega)\,\mathrm{d}\Omega\right]-H(t)\frac{\mathrm{d}}{\mathrm{d}t}\left[\int_{\Omega_1}^{\Omega_2}e^{-t\Omega}\kappa_\nu(\Omega)\,\mathrm{d}\Omega\right]$$
$$=\frac{\kappa_0\tau_\epsilon^\alpha}{\tau_\sigma^\alpha}\delta(t)-\kappa_0\left(1-\tau_\epsilon^\alpha/\tau_\sigma^\alpha\right)H(t)\frac{\mathrm{d}}{\mathrm{d}t}E_{\alpha,1}[-(t/\tau_\sigma)^\alpha]. \quad (18)$$

The problem thus reduces to selection of a $\kappa_\nu(\Omega)$ distribution for which equality (18) is true. As pointed out in the Appendix, the Mittag-Leffler function may be written on an integral form [Eq. (A5)]. This inspires the choice of a the distribution $\kappa_\nu(\Omega)$ as

$$\kappa_{\nu\mathrm{ML}}(\Omega)\triangleq\kappa_0\left(1-\tau_\epsilon^\alpha/\tau_\sigma^\alpha\right)f_{\alpha,1}\left(\Omega,\tau_\sigma^{-\alpha}\right)$$
$$=\frac{1}{\pi}\frac{\kappa_0\left(\tau_\sigma^\alpha-\tau_\epsilon^\alpha\right)\Omega^{\alpha-1}\sin(\alpha\pi)}{(\tau_\sigma\Omega)^{2\alpha}+2(\tau_\sigma\Omega)^\alpha\cos(\alpha\pi)+1}, \quad (19)$$

where $f_{\alpha,1}(\Omega, a)$ was inserted from Eq. (A7). Under the condition that $\Omega_1=0$ and $\Omega_2\to\infty$, this κ_ν distribution makes NSW generalized compressibility (6) become

$$\kappa_{\mathrm{ML}}(t)\triangleq\delta(t)\left[\kappa_0-\kappa_0\left(1-\tau_\epsilon^\alpha/\tau_\sigma^\alpha\right)\int_{\Omega_1=0}^{\Omega_2\to\infty}f_{\alpha,1}\left(\Omega,\tau_\sigma^{-\alpha}\right)\mathrm{d}\Omega\right]$$
$$-\kappa_0\left(1-\tau_\epsilon^\alpha/\tau_\sigma^\alpha\right)H(t)$$
$$\times\frac{\mathrm{d}}{\mathrm{d}t}\left[\int_{\Omega_1=0}^{\Omega_2\to\infty}e^{-t\Omega}f_{\alpha,1}\left(\Omega,\tau_\sigma^{-\alpha}\right)\mathrm{d}\Omega\right]. \quad (20)$$

Use of Eqs. (A4) and (A8), demonstrates that this equals

$$\kappa_{\mathrm{ML}}(t)=\delta(t)\left[\kappa_0-\kappa_0\left(1-\tau_\epsilon^\alpha/\tau_\sigma^\alpha\right)\right]$$
$$-\kappa_0\left(1-\tau_\epsilon^\alpha/\tau_\sigma^\alpha\right)H(t)\frac{\mathrm{d}}{\mathrm{d}t}E_{\alpha,1}[-(t/\tau_\sigma)^\alpha], \quad (21)$$

which after a minor algebraic reorganization is identified to be equal to the fractional Zener generalized compressibility $\kappa_Z(t)$ as given by Eq. (13). This thus demonstrates that for $\kappa_\nu(\Omega)=\kappa_{\nu\mathrm{ML}}(\Omega)$ as given by Eq. (19), with $\Omega\in[0,\infty]$, the NSW and the fractional Zener generalized compressibilities are identical. Therefore both models then have the same dispersion relation between k and ω. Because of the Fourier transform relation between the dispersion relation and the wave equation, this implies that the NSW wave equation then equals fractional Zener wave equation (14).

Using Eq. (5) and the selected distribution $\kappa_{\nu\mathrm{ML}}(\Omega)$, the frequency-domain generalized compressibility corresponding to Eq. (20) becomes

$$\kappa_{\mathrm{ML}}(t)\triangleq\kappa_0-\frac{i\omega\kappa_0\left(\tau_\sigma^\alpha-\tau_\epsilon^\alpha\right)}{\pi}\int_0^\infty\frac{1}{\Omega+i\omega}$$
$$\times\frac{\Omega^{\alpha-1}\sin(\alpha\pi)}{(\tau_\sigma\Omega)^{2\alpha}+2(\tau_\sigma\Omega)^\alpha\cos(\alpha\pi)+1}\mathrm{d}\Omega, \quad (22)$$

which from Eqs. (2) and (3) gives the attenuation

$$\alpha_{k,\mathrm{ML}}(\omega)\triangleq-\Im\left\{\omega\sqrt{\rho_0\kappa_{\mathrm{ML}}(\omega)}\right\} \quad (23)$$

and the speed of sound

$$c_{\mathrm{ML}}(\omega)\triangleq\frac{1}{\Re\sqrt{\rho_0\kappa_{\mathrm{ML}}(\omega)}}. \quad (24)$$

For notational convenience, the special case of the NSW model where the continuum of relaxation mechanisms distributed in the frequency interval $\Omega\in[0,\infty]$ following $\kappa_\nu(\Omega)$ as given by Eq. (19) is for the remainder of this paper denoted the ML-NSW model. As shown analytically previously, the ML-NSW model equals the fractional Zener model.

Inspired by the findings that adequate fits to power-law attenuation may be attained within limited frequency intervals using a few discrete relaxation processes,[6,7] we explore in the following the effect of letting a continuum of relaxation mechanisms populate only a bounded frequency interval, rather than the entire $\Omega\in[0,\infty]$ region. The case of a ML-NSW model for a limited frequency interval $\Omega\in[\Omega_1,\Omega_2]$ is for the remainder of this paper denoted the approximate ML-NSW model. In order to study the influence such bounded spectra have on the attenuation and the sound speed dispersion, the numerical examples below also cover the approximate ML-NSW case.

One may note that κ_∞ as given in Eq. (7) is finite for both the full ML-NSW and for the approximate ML-NSW models. It may actually be evaluated analytically as[24]

$$\kappa_{\infty,\mathrm{ML}}\triangleq\frac{(\tau_\epsilon/\tau_\sigma)^\alpha}{2\pi\alpha}\left\{\angle\left[\Omega_1^\alpha+\frac{e^{i\pi\alpha}}{\tau_\sigma^\alpha}\right]-\angle\left[\Omega_1^\alpha+\frac{e^{-i\pi\alpha}}{\tau_\sigma^\alpha}\right]\right.$$
$$\left.-\angle\left[\Omega_2^\alpha+\frac{e^{i\pi\alpha}}{\tau_\sigma^\alpha}\right]+\angle\left[\Omega_2^\alpha+\frac{e^{-i\pi\alpha}}{\tau_\sigma^\alpha}\right]\right\}. \quad (25)$$

Following a similar line as in Ref. 1 for HF and LF approximation, one may conclude that the attenuation for the approximate ML-NSW model is constant at high frequencies $\Omega_1<\Omega_2\ll\omega$ and proportional to ω^2 for low frequencies $\omega\ll\Omega_1<\Omega_2$. The speed of sound is constant for both regimes, being greater for the HF than for the LF case.

Figure 1 compares attenuation curves given by the approximate ML-NSW model in Eq. (23) to the attenuation

given by the fractional Zener model from Eq. (16), and Fig. 2 displays the corresponding frequency-dependent speed of sound given by Eqs. (24) and (17), respectively. The integral over $\Omega \in [\Omega_1, \Omega_2]$ in the calculation of $\kappa_{\mathrm{ML}}(\omega)$ is evaluated numerically using the recursive adaptive Simpson quadrature method.

III. NUMERICAL EXAMPLE

Below follows an example where the ML-NSW model is fitted to the attenuation power-law $\alpha_k \propto \omega^{1.1}$ between 100 kHz and 30 MHz. This example is relevant for medical ultrasound imaging and the chosen medium properties and power law are equal to those used by Yang and Cleveland in Ref. 7. They fitted two relaxation terms and a thermoviscous component to an approximate $\alpha_k \propto \omega^{\eta}$ power law using Eq. (1). Table I lists the parameters of the medium and the desired attenuation model. Note that there is a typographical error in Eq. (13) of Ref. 7: the second relaxation parameter should be $(c'/c_0)_{R2} = 1.6597 \times 10^{-2}$ (R. O. Cleveland, personal communication). In the following, the corresponding ML-NSW model parameters are calculated by first choosing the fractional derivative parameter α so that the low-frequency (LF) approximation of the fractional Zener attenuation power law,

$$\alpha_k(\omega) \approx \frac{\omega^{1+\alpha}}{2c_0}\left(\tau_\sigma^\alpha - \tau_\epsilon^\alpha\right)\sin\frac{\pi\alpha}{2}, \tag{26}$$

gives $\alpha_k \propto \omega^{1.1}$. Then τ_ϵ is chosen high enough to ensure the model frequency band to be within the LF regime. Finally, the difference $\tau_\sigma^\alpha - \tau_\epsilon^\alpha$ is adjusted to ensure $\alpha_k(\omega) = 0.3$ dB/MHz/cm at $f = 1$ MHz.

Figure 3 compares the resulting attenuation due to the ML-NSW model and the corresponding fractional Zener model to the Yang and Cleveland fit. The ML-NSW and fractional Zener model parameters used to yield the desired attenuation power law plotted in the figure are listed in Table II.

IV. DISCUSSION AND CONCLUDING REMARKS

This paper supports the commonly recognized hypothesis[25] that a continuum of multiple relaxation processes gives rise to an attenuation power law $\alpha_k \propto \omega^{\eta}$ in complex media. For the appropriate weighting of the relaxation processes, the fractional Zener model is obtained from the NSW multiple relaxation framework of Ref. 1. The advantages of the fractional Zener model is that it fits measurements well and it is characterized by a relatively small number of parameters, whereas the NSW model is more intuitive as it does not comprise fractional derivatives. It is also better rooted in fundamental physics.

As stated in Ref. 1, a multitude of processes originating from, e.g., chemical, structural, and vibrational mechanisms, may be described by the same kind of linearized partial

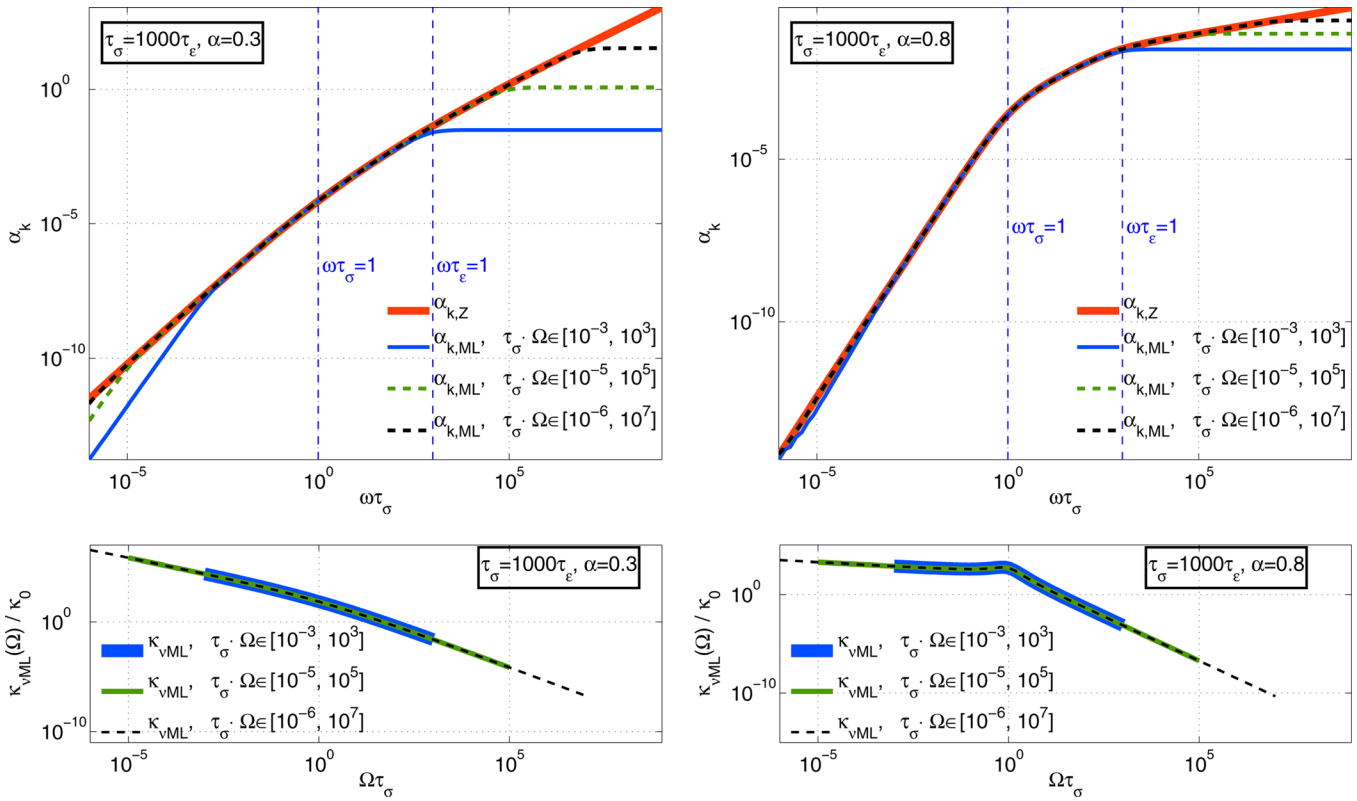

FIG. 1. (Color online) Top panels: Frequency-dependent attenuation for $\tau_\sigma = 1000\tau_\epsilon$ with the fractional derivative orders $\alpha = 0.3$ (top left), and $\alpha = 0.8$ (top right). The attenuation curves displayed show $\alpha_{k,Z}(\omega)$ from Eq. (16) as predicted by the fractional Zener model, and as predicted for the approximate ML-NSW model by $\alpha_{k,\mathrm{ML}}(\omega)$ in Eq. (23) for a set of Ω_1 and Ω_2 choices as displayed in the legends. The horizontal axis represents normalized frequency. For visualization convenience, each absorption curve is normalized to $\alpha_k = 1$ at $\omega\tau_\sigma = 1$. Bottom panels: The corresponding normalized effective compressibilities $\kappa_{\nu\mathrm{ML}}(\Omega)$ of the continuum of relaxation processes as a function of normalized relaxation frequency $\Omega\cdot\tau_\sigma$ for $\alpha = 0.3$ (bottom left), and $\alpha = 0.8$ (bottom right) of the approximate ML-NSW model with Ω limits as described in the legends.

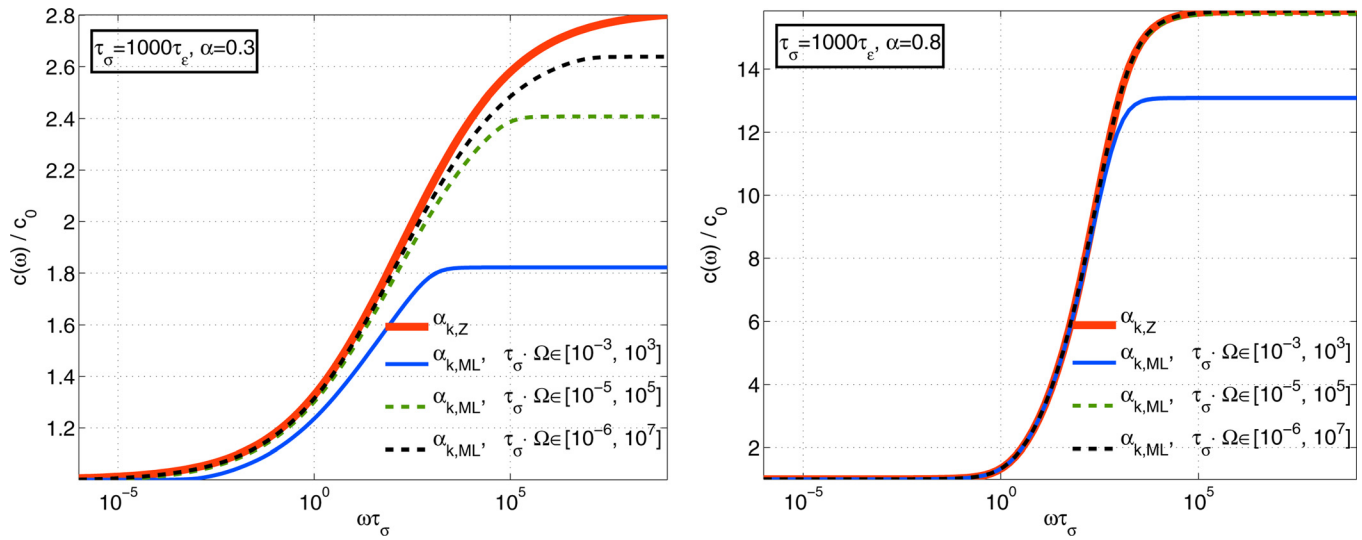

FIG. 2. (Color online) Frequency-dependent speed of sound for $\tau_\sigma = 1000\tau_\epsilon$ with the fractional derivative orders $\alpha = 0.3$ (left pane), and $\alpha = 0.8$ (right pane). The curves display $c_Z(\omega)$ from Eq. (17) as predicted by the fractional Zener model, and as predicted by $c_{\mathrm{ML}}(\omega)$ in Eq. (24) for a set of Ω_1 and Ω_2 choices as displayed in the legends. The horizontal axis represents normalized frequency.

differential relaxation equation. The current paper does not explain or suggest what kind of mechanisms would cause the continuum of relaxations having the compressibility contribution following $\kappa_\nu(\Omega)$ as proposed in Eq. (19). However, the fact that this choice is shown to make the attenuation follow the often observed power law, infers that the model presumably is an adequate description of the relaxations taking place in complex media. The high-frequency asymptote of the compressibility distribution $\kappa_{\nu\mathrm{ML}}(\Omega)$ in Eq. (19) is proportional to $\Omega^{-\alpha-1}$. This is illustrated in the bottom panes of Fig. 1, where the high-frequency tails fall off linearly in the log–log plots. The distribution of compressibilities thus has self-similar, i.e., fractal, properties. Such fall-off also arises for Levy α-stable distributions. Whether this characteristic reveals information about the nature of the underlying physical relaxation processes is subject to future study. It is tempting to surmise that the appearance of compressibility distributions like Eq. (19) is due to properties of the medium microstructure.

The numerical examples of Figs. 1 and 3 suggest that the approximate ML-NSW model gives the same attenuation as the fractional Zener model but within a limited frequency band. The examples also indicate that the width of the frequency band where the approximate ML-NSW gives the same attenuation as the fractional Zener model is related to the width of the populated relaxation frequency band $\Omega \in [\Omega_1, \Omega_2]$. Increasing this interval would thus expand the frequency interval where the fractional Zener wave equation is valid.

Simulations using fractional wave equations involve numerical evaluation of the fractional derivative and/or the Mittag-Leffler function. It is an evolving research field where some work is based on wave equations with fractional time-derivatives, e.g., Caputo *et al.*[26] and Wismer,[12] whereas others utilize space-fractional derivatives, e.g., Carcione[27] and Treeby and Cox.[9] This paper provides physical arguments for use of the first approach with time-fractional operators. However, further development of such simulations is considered outside the scope of this work.

TABLE I. Medium parameters for the attenuation power-law fit, similar to the Yang and Cleveland parameters in Ref. 7.

Equilibrium speed of sound, c_0 (m/s)	1540
Density, ρ_0 (kg/m^3)	1050
Zero-frequency compressibility, $\kappa_0 = 1/(c_0^2\rho_0)$ (Pa^{-1})	4.0158×10^{-10}
Wanted attenuation at 1 MHz, α_0 (dB/MHz/cm)	0.3
Wanted attenuation power-law exponent, η	1.1

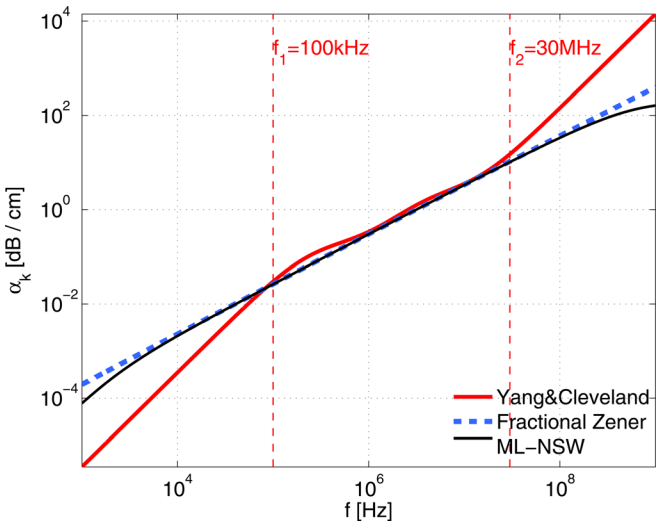

FIG. 3. (Color online) Comparison of resulting attenuation modeled in Ref. 7 (thick solid line), fractional Zener model (dashed line), and the approximate ML-NSW model by use of $\kappa_{\nu\mathrm{ML}}(\Omega)$ (thin solid line) of Eq. (19). The medium parameters are displayed in Table I. The fractional Zener and approximate ML-NSW parameters are listed in Table II.

TABLE II. Fitted fractional Zener and ML-NSW model parameters corresponding to the Yang and Cleveland attenuation properties as reproduced in Table I. The resulting attenuation is displayed in Fig. 3.

Fractional derivative order, α	0.1
Zener retardation time, τ_ϵ (s)	1.000×10^{-12}
Zener relaxation time, τ_σ (s)	1.829×10^{-12}
Zero-freq. compressibility, $\kappa_0 = 1/(c_0^2\rho_0)$ (Pa^{-1})	4.0158×10^{-10}
Relaxation distribution interval, $[\Omega_1, \Omega_2]$ (Hz)	$[10^4, 5 \times 10^9]$

The model previously considered by Berkhoff *et al.*[18] where a continuum of relaxation mechanisms of equal compressibility is logarithmically distributed within the angular frequency interval $\Omega \in [\omega_L, \omega_H]$, may be seen as a special case of the model presented in the current paper. They use $\tau_\nu = e^{-B\nu}/\Omega_0$ and $\kappa_\nu = \kappa_{\text{ref}}$, which gives the equivalent to Eq. (5) as

$$\begin{aligned}\kappa(\omega) &= \kappa_0 - i\omega\kappa_{\text{ref}} \int_{\Omega_1}^{\Omega_2} \frac{1}{\Omega_0 e^{B\Omega} + i\omega} \mathrm{d}\Omega \\ &= \kappa_0 - \frac{i\omega\kappa_{\text{ref}}}{B} \int_{\omega_L = \Omega_0 e^{B\Omega_1}}^{\omega_H = \Omega_0 e^{B\Omega_2}} \frac{1}{\Omega} \cdot \frac{1}{\Omega + i\omega} \mathrm{d}\Omega \end{aligned} \tag{27}$$

from which one may identify the choice $\kappa_\nu(\Omega) = \kappa_{\text{ref}}/(B\Omega)$ with $\Omega_{1,2} = B^{-1}\ln(\omega_{L,H}/\Omega_0)$ for the Berkhoff *et al.* approach.

The path followed in the present paper for connection between a certain choice of $\kappa_\nu(\Omega)$ with a continuum of NSW relaxations and the fractional Zener model may be followed also for deduction of other fractional (and nonfractional) constitutive models and the related wave equations from the NSW relaxation model. An obvious example is that the fractional Kelvin–Voigt model and corresponding wave equation[14] is obtained if τ_ϵ is set to 0 for $\kappa_{\nu\text{ML}}(\Omega)$ in Eq. (19). Another such straightforward example is the fractional Maxwell model which agrees with $\tau_\sigma = 0$ in $\kappa_{\nu\text{ML}}(\Omega)$. Yet another example is for the case of $\alpha = 1$ in $\kappa_{\nu\text{ML}}(\Omega)$, which makes $f_{\alpha,1}(\Omega, \tau_\sigma^{-\alpha})$ approach Dirac's delta function. The generalized compressibility corresponding to this equals the nonfractional Zener constitutive model generalized compressibility, which gives a wave equation with the attenuation power-law exponent $\eta = 2$ in the LF regime (i.e., viscous-like), 1/2 in an intermediate regime, and 1 in the HF regime. A rigorous analysis of different realizations of $\kappa_{\nu\text{ML}}(\Omega)$, their connected constitutive stress–strain models, and the resulting lossy wave equations are suggested as future work to follow up the present paper. Hopefully, the developments compiled in this paper will bring about a wider acceptance for use of fractional wave equations amongst workers in the field of acoustical modeling.

ACKNOWLEDGMENTS

We would like to thank Professor Robin O. Cleveland, Boston University, and Professor Robert C. Waag, University of Rochester, for interesting discussions on relaxation models. This research was partly supported by the "High Resolution Imaging and Beamforming" project of the Norwegian Research Council.

APPENDIX: THE MITTAG-LEFFLER FUNCTION

1. Definition and Fourier transform

The one-parameter Mittag-Leffler function was introduced by Gösta Mittag-Leffler.[28] It may be regarded as a generalization of the exponential function. A two-parameter analogy was presented by Wiman,[29] and may be written in the form

$$E_{\alpha,\beta}(t) \triangleq \sum_{n=0}^{\infty} \frac{t^n}{\Gamma(\alpha n + \beta)}, \tag{A1}$$

where Γ denotes the Euler gamma function and the parameters are commonly restricted to $\{\alpha, \beta\} \in \mathbb{C}$, $\Re\{\alpha, \beta\} > 0$, and the argument $t \in \mathbb{C}$. The one-parameter Mittag-Leffler function $E_\alpha(t)$ equals the two-parameter $E_{\alpha,\beta}(t)$ of Eq. (A1) with $\beta = 1$. See Ref. 30 for a comprehensive review of Mittag-Leffler function properties.

A useful Fourier transform pair involving the Mittag-Leffler function is[21]

$$\mathcal{F}\{H(t)t^{\beta-1}E_{\alpha,\beta}(-\alpha t^\alpha)\}(\omega) = \frac{(i\omega)^{\alpha-\beta}}{a + (i\omega)^\alpha}, \tag{A2}$$

which is equivalent to

$$\mathcal{F}\left\{\frac{\mathrm{d}}{\mathrm{d}t}\left[H(t)t^{\beta-1}E_{\alpha,\beta}(-\alpha t^\alpha)\right]\right\}(\omega) = \frac{(i\omega)^{\alpha-\beta+1}}{a + (i\omega)^\alpha}. \tag{A3}$$

Another useful relation which follows from the Mittag-Leffler function definition (A1) is

$$t^{\alpha-1}E_{\alpha,\alpha}(-at^\alpha) = -a^{-1}\frac{\mathrm{d}}{\mathrm{d}t}E_{\alpha,1}(-at^\alpha). \tag{A4}$$

2. Integral representation

The Mittag-Leffler related function $t^{\beta-1}E_{\alpha,\beta}(-\alpha t^\alpha)$ may for $0 < a \leq 1$ be written in integral form:[31,32]

$$t^{\beta-1}E_{\alpha,\beta}(-at^\alpha) = \int_0^\infty e^{-\Omega t} f_{\alpha,\beta}(\Omega, a)\mathrm{d}\Omega, \tag{A5}$$

where

$$f_{\alpha,\beta}(\Omega, a) = \frac{\Omega^{\alpha-\beta}}{\pi} \frac{a\sin[(\beta-\alpha)\pi] + \Omega^\alpha \sin(\beta\pi)}{\Omega^{2\alpha} + 2a\Omega^\alpha\cos(\alpha\pi) + a^2}. \tag{A6}$$

For $\beta = 1$,

$$f_{\alpha,1}(\Omega, a) = \frac{1}{\pi} \frac{a\Omega^{\alpha-1}\sin(\alpha\pi)}{\Omega^{2\alpha} + 2a\Omega^\alpha\cos(\alpha\pi) + a^2}, \tag{A7}$$

which has a finite integral from 0 to ∞ given by

$$\int_0^\infty f_{\alpha,1}(\Omega, a)\mathrm{d}\Omega = E_{\alpha,1}(0) = 1. \tag{A8}$$

The function $f_{\alpha,1}(1,\Omega)$ may be considered as a random variable density corresponding to a Mittag-Leffler distribution function $F_\alpha(x) = 1 - E_{\alpha,1}(-x^\alpha)$.[33]

A noteworthy observation regarding integral (A8) between the limits $\Omega = \Omega_1$ and Ω_2 is that using the variable change $u = \Omega^\alpha$, it may instead be written as

$$\frac{a\sin(\alpha\pi)}{\pi}\int_{\Omega_1}^{\Omega_2}\frac{\Omega^{\alpha-1}}{\Omega^{2\alpha}+2a\Omega^\alpha\cos(\alpha\pi)+a^2}\,\mathrm{d}\Omega = \frac{a\sin(\alpha\pi)}{\alpha\pi}\int_{\Omega_1^\alpha}^{\Omega_2^\alpha}\frac{1}{u^2+2au\cos(\alpha\pi)+a^2}\,\mathrm{d}u. \tag{A9}$$

[1]A. I. Nachman, J. F. Smith III, and R. C. Waag, "An equation for acoustic propagation in inhomogeneous media with relaxation losses," J. Acoust. Soc. Am. **88**, 1584–1595 (1990).
[2]K. Waters, J. Mobley, and J. Miller, "Causality-imposed (Kramers–Kronig) relationships between attenuation and dispersion," IEEE Trans. Ultrason. Ferroelectr., Freq. Control **52**, 822–833 (2005).
[3]H. Bass, L. Sutherland, A. Zuckerwar, D. Blackstock, and D. Hester, "Atmospheric absorption of sound: Further developments," J. Acoust. Soc. Am. **97**, 680–683 (1995).
[4]M. Ainslie and J. McColm, "A simplified formula for viscous and chemical absorption in sea water," J. Acoust. Soc. Am. **103**, 1671–1672 (1998).
[5]T. Szabo and J. Wu, "A model for longitudinal and shear wave propagation in viscoelastic media," J. Acoust. Soc. Am. **107**, 2437–2446 (2000).
[6]M. Tabei, T. D. Mast, and R. C. Waag, "Simulation of ultrasonic focus aberration and correction through human tissue," J. Acoust. Soc. Am. **113**, 1166–1176 (2003).
[7]X. Yang and R. O. Cleveland, "Time domain simulation of nonlinear acoustic beams generated by rectangular pistons with application to harmonic imaging," J. Acoust. Soc. Am. **117**, 113–123 (2005).
[8]W. Chen and S. Holm, "Fractional Laplacian time-space models for linear and nonlinear lossy media exhibiting arbitrary frequency power-law dependency," J. Acoust. Soc. Am. **115**, 1424–1430 (2004).
[9]B. Treeby and B. Cox, "Modeling power law absorption and dispersion for acoustic propagation using the fractional Laplacian," J. Acoust. Soc. Am. **127**, 2741–2748 (2010).
[10]M. Caputo, "Linear models of dissipation whose Q is almost frequency independent-II," Geophys. J. R. Astron. Soc. **13**, 529–539 (1967).
[11]W. Chen and S. Holm, "Modified Szabo's wave equation models for lossy media obeying frequency power law," J. Acoust. Soc. Am. **114**, 2570–2574 (2003).
[12]M. Wismer, "Finite element analysis of broadband acoustic pulses through inhomogenous media with power law attenuation," J. Acoust. Soc. Am. **120**, 3493–3502 (2006).
[13]J. F. Kelly, R. J. McGough, and M. M. Meerschaert, "Analytical time-domain Green's functions for power-law media," J. Acoust. Soc. Am. **124**, 2861–2872 (2008).
[14]S. Holm and R. Sinkus, "A unifying fractional wave equation for compressional and shear waves," J. Acoust. Soc. Am. **127**, 542–548 (2010).
[15]S. Holm and S. P. Näsholm, "A causal and fractional all-frequency wave equation for lossy media," J. Acoust. Soc. Am. **130**, 2195–2202 (2011).
[16]F. Prieur and S. Holm, "Nonlinear acoustics with fractional loss operators," J. Acoust. Soc. Am. **130**, 1125–1132 (2011).
[17]J. Kelly and R. McGough, "Fractal ladder models and power law wave equations," J. Acoust. Soc. Am. **126**, 2072–2081 (2009).
[18]A. P. Berkhoff, J. M. Thijssen, and R. J. F. Homan, "Simulation of ultrasonic imaging with linear arrays in causal absorptive media," Ultrasound Med. Biol. **22**, 245–259 (1996).
[19]R. L. Bagley and P. J. Torvik, "Fractional calculus—a different approach to the analysis of viscoelastically damped structures," AIAA J. **21**, 741–748 (1983).
[20]N. H. Abel, "Auflösung einer mechanischen Aufgabe (Resolution of a mechanical problem)," J. Reine. Angew. Math. 153–157 (1826).
[21]I. Podlubny, *Fractional Differential Equations* (Academic, New York, 1999), Chaps. 1 and 2.
[22]R. Bagley and P. Torvik, "On the fractional calculus model of viscoelastic behavior," J. Rheol. **30**, 133–155 (1986).
[23]W. Glöckle and T. Nonnenmacher, "Fractional integral operators and Fox functions in the theory of viscoelasticity," Macromolecules **24**, 6426–6434 (1991).
[24]I. S. Gradshteyn and I. M. Ryzhik, *Table of Integrals, Series, and Products*, 7th ed. (Academic, Burlington, MA, 2007), Chap. 2.
[25]B. A. J. Angelsen, *Ultrasound Imaging*, Waves, Signals and Signal Processing Vol. 1 (Emantec, Trondheim, Norway, 2000), Chap. 4.
[26]M. Caputo, J. M. Carcione, and F. Cavallini, "Wave simulation in biologic media based on the Kelvin–Voigt fractional-derivative stress–strain relation," Ultrasound Med. Biol. **37**, 996–1004 (2011).
[27]J. M. Carcione, "A generalization of the Fourier pseudospectral method," Geophysics **75**, A53–A56 (2010).
[28]M. G. Mittag-Leffer, "Sur la nouvelle fonction $E_\alpha(x)$ [On the new function $E_\alpha(x)$]," C. R. Acad. Sci. Paris **137**, 554–558 (1903).
[29]A. Wiman, "Über den Fundamentalsatz in der Theorie der Funktionen $E_\alpha(x)$ [About the fundamental theorem in the theory of the function $E_\alpha(x)$]," Acta Math. **29**, 191–201 (1905).
[30]H. J. Haubold, A. M. Mathai, and R. K. Saxena, "Mittag-Leffler functions and their applications," J. Appl. Math. **2011**, 1–51 (2011).
[31]M. M. Djrbashian, *Integral Transforms and Representations of Functions in the Complex Domain* (Nauka, Moscow, USSR, 1966), Chaps. 3 and 4 (in Russian).
[32]M. M. Djrbashian, *Harmonic Analysis and Boundary Value Problems in the Complex Domain* (Birkhauser, Basel, Switzerland, 1993), Chap. 1.
[33]R. N. Pillai, "On Mittag-Leffler and related distributions," Ann. Inst. Stat. Math. **42**, 157–161 (1990).